

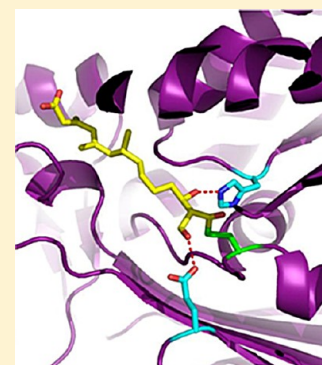
# Biochemical and Structural Basis for Inhibition of *Enterococcus faecalis* Hydroxymethylglutaryl-CoA Synthase, *mvaS*, by Hymeglusin

D. Andrew Skaff,<sup>†</sup> Kasra X. Ramyar,<sup>‡</sup> William J. McWhorter,<sup>‡</sup> Michael L. Barta,<sup>‡</sup> Brian V. Geisbrecht,<sup>\*,‡</sup> and Henry M. Mizioro<sup>\*,†</sup>

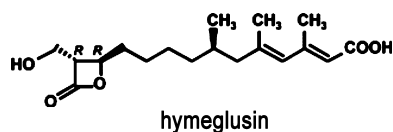
<sup>†</sup>Division of Molecular Biology and Biochemistry and <sup>‡</sup>Division of Cell Biology and Biophysics, University of Missouri—Kansas City, Kansas City, Missouri 64110, United States

## S Supporting Information

**ABSTRACT:** Hymeglusin (1233A, F244, L-659-699) is established as a specific  $\beta$ -lactone inhibitor of eukaryotic hydroxymethylglutaryl-CoA synthase (HMGCS). Inhibition results from formation of a thioester adduct to the active site cysteine. In contrast, the effects of hymeglusin on bacterial HMG-CoA synthase, *mvaS*, have been minimally characterized. Hymeglusin blocks growth of *Enterococcus faecalis*. After removal of the inhibitor from culture media, a growth curve inflection point at 3.1 h is observed (vs 0.7 h for the uninhibited control). Upon hymeglusin inactivation of purified *E. faecalis* *mvaS*, the thioester adduct is more stable than that measured for human HMGCS. Hydroxylamine cleaves the thioester adduct; substantial enzyme activity is restored at a rate that is 8-fold faster for human HMGCS than for *mvaS*. Structural results explain these differences in enzyme–inhibitor thioester adduct stability and solvent accessibility. The *E. faecalis* *mvaS*–hymeglusin cocrystal structure (1.95 Å) reveals virtually complete occlusion of the bound inhibitor in a narrow tunnel that is largely sequestered from bulk solvent. In contrast, eukaryotic (*Brassica juncea*) HMGCS binds hymeglusin in a more solvent-exposed cavity.



Hymeglusin {(2*E*,4*E*,7*R*)-11-[(2*R*,3*R*)-3-(hydroxymethyl)-4-oxooxetan-2-yl]-3,5,7-trimethylundeca-2,4-dienoic acid} was chemically characterized by Aldridge et al.<sup>1</sup> and described as an antibiotic, but its biological properties were not reported. Tomoda et al.<sup>2</sup> subsequently demonstrated hymeglusin's antimicrobial activity against several fungi and bacteria.



After Mizioro and Behnke<sup>3,4</sup> identified 3-chloropropionyl-CoA as a mechanism-based inactivator of animal HMG-CoA synthase (EC 4.1.3.5), hymeglusin was identified as the first natural product that specifically inhibits this cholesterologenic enzyme.<sup>5,6</sup> This led to an expanded effort in characterizing hymeglusin inhibition of eukaryotic cholesterol biosynthesis<sup>6,7</sup> and of eukaryotic HMG-CoA synthase.<sup>8</sup> Both 3-chloropropionyl-CoA and hymeglusin target the active site cysteine involved in forming the two reaction intermediates, which are thioester adducts of enzyme to acetyl or HMG-CoA groups (Schemes 1 and 2).

The confirmation of the active site function of the cysteine targeted by these inactivators was provided by the demonstration<sup>9</sup> that alanine or serine substitution of this residue produced an enzyme that was devoid of catalytic activity and unable to form the covalent reaction intermediates. More recently, Pojer et al.<sup>10</sup> reported the structure of an adduct of *Brassica juncea* HMG-CoA synthase with hymeglusin. These

results showed that the inhibitor's extended aliphatic chain bound in a funnel-shaped cavity of this plant enzyme and confirmed the formation of a thioester between the inhibitor's  $\beta$ -lactone and the active site cysteine.

While hymeglusin was originally described as an antibiotic, little is known about its interaction with *mvaS*, the bacterial HMG-CoA synthase. This report characterizes the inhibitor's effect on *Enterococcus faecalis* and on isolated *E. faecalis* *mvaS*. Differences between the persistence of the inhibition observed for bacterial cells in light of analogous observations documented for animal cells<sup>7</sup> prompted comparison of the enzyme–inactivator adducts for *E. faecalis* and human enzymes. The results suggested possible differences in the hymeglusin binding sites. Crystallization of hymeglusin-inactivated *mvaS* allowed a test of this hypothesis. The complementary biochemical and structural results of these studies are presented.

## EXPERIMENTAL PROCEDURES

**Materials.** Acetyl-CoA and acetoacetyl-CoA were synthesized using acetic anhydride and diketene, respectively, according to the procedure of Simon and Shemin.<sup>11</sup> Hymeglusin (L-659-699) was a generous gift from M. D. Greenspan (Merck Research Laboratories). Hydroxylamine hydrochloride was purchased from Eastman Laboratory

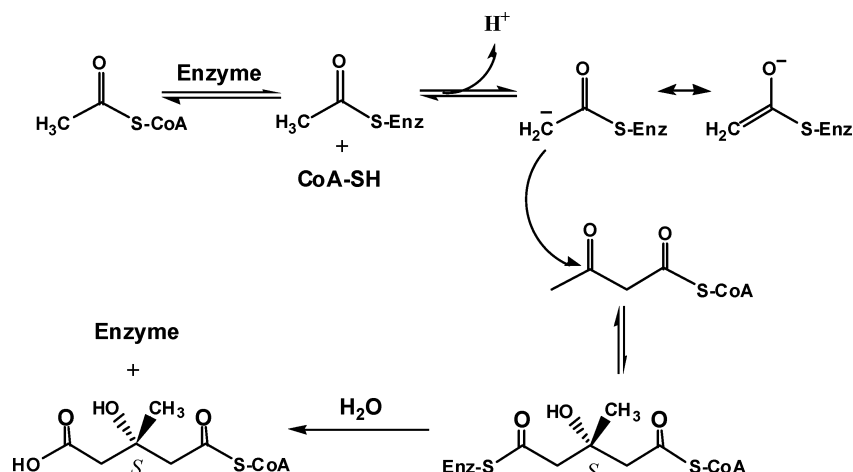
Received: January 10, 2012

Revised: April 16, 2012

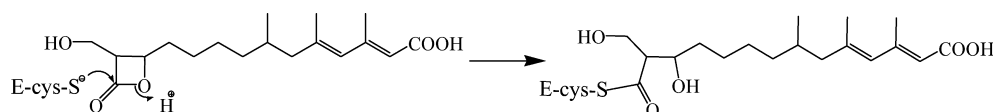
Published: April 17, 2012



Scheme 1. HMG-CoA Synthase (mvaS) Reaction



Scheme 2. Reaction of Hymeglusin with the Active Site Cysteine of HMG-CoA Synthase (mvaS)



Chemicals. Other biological and chemical products used in these studies were reagent grade materials purchased from Fisher Scientific or Sigma-Aldrich.

**Cloning, Overexpression, and Purification of *E. faecalis* mvaS.** A gene fragment encoding the entire mvaS open reading frame (residues 1–383) was amplified from *E. faecalis* genomic DNA by polymerase chain reaction, digested with *Bam*HI and *Not*I endonucleases, and subcloned into the corresponding restriction sites of the prokaryotic overexpression vector pT7HMT.<sup>12</sup> This vector directs IPTG-inducible expression of an N-terminally hexahistidine-tagged form of the mvaS protein, which can be digested from the affinity tag following treatment with TEV protease. Following confirmation of the mvaS sequence, the plasmid described above was transformed into *Escherichia coli* BL21(DE3) cells. Selection of positive transformants, bacterial growth, and induction of protein overexpression were conducted according to previously published methods.<sup>13</sup>

Soluble, tagged *E. faecalis* mvaS was isolated from 1 L of induced *E. coli* cells through a combination of affinity and ion-exchange chromatographies. Briefly, the cells were resuspended and homogenized by microfluidization, and a soluble extract was prepared by high-speed centrifugation as described by Barta et al.<sup>13</sup> The tagged mvaS enzyme was then recovered from this supernatant using a Ni<sup>2+</sup>-NTA Sepharose column (GE Biosciences), again as previously described.<sup>12</sup> Upon elution from the affinity column, recombinant TEV protease was used to digest the mvaS enzyme from its affinity tag;<sup>12</sup> however, a GSTGS sequence remains at the N-terminus of the enzyme as an artifact of the subcloning procedure. Following buffer exchange into 20 mM Tris (pH 8.0), final purification to apparent homogeneity was achieved by Resource Q anion-exchange chromatography (GE Biosciences). The purified mvaS was concentrated to 5 mg/mL, buffer exchanged into 10 mM Tris (pH 7.5) and 50 mM NaCl, and stored at 4 °C for further use.

**Growth Inhibition of the *E. faecalis* Culture by Hymeglusin.** Two samples (10 mL) of sterile LB culture

media, containing either 0 or 25  $\mu$ M hymeglusin, were inoculated with 200  $\mu$ L of an overnight culture of *E. faecalis*. Samples were incubated with shaking for 3 h at 37 °C. A 3 mL aliquot of each culture was centrifuged at 3000g for 5 min to pellet bacteria before resuspension in either 3 mL of fresh LB or fresh LB containing 25  $\mu$ M hymeglusin. At 30 min intervals the absorbance of each culture was measured at 600 nm.

**Kinetic Characterization of Inhibition of *E. faecalis* mvaS by Hymeglusin.** Enzyme activity was measured at 412 nm by the DTNB method of Skaff and Mizioroko.<sup>14</sup> Purified mvaS (48 nM) was incubated with hymeglusin (75–600 nM) in 100 mM Tris-HCl (pH 8.0). The reaction was performed at 18 °C to allow measurement of activity at an adequate number of time points while maintaining elevated hymeglusin/enzyme concentration ratios. At the specified time points, 400  $\mu$ M acetyl-CoA (approximately  $K_m$  level) was added to the incubation mix to acetylate the free enzyme and protect against further formation of any hymeglusin adduct. Acetoacetyl-CoA (7  $\mu$ M) was then added to initiate the measurement of enzyme activity, which was performed in the presence of 0.2 mM DTNB. The data, which indicated time-dependent loss of activity, were fit to semilog plots of percent residual activity versus time using a linear model and Microsoft Excel; correlation coefficients ranged from 0.970 to 0.995. Nonlinear regression fits (GraphPad Prism 4) of the data indicated a  $k_{inact}$  of  $3.5 \pm 0.6 \text{ min}^{-1}$  and a  $K_i$  of  $700 \pm 18.5 \text{ nM}$ .

**Recovery of HMGCS and mvaS Activity from Hymeglusin Inhibition.** Purified human HMGCS<sup>14</sup> or *E. faecalis* mvaS samples (9  $\mu$ M) were incubated with 20  $\mu$ M hymeglusin at room temperature in 0.1 M Tris-HCl (pH 8.0) for 1 h. After this incubation period, each protein sample retained <10% of the residual activity as determined by the DTNB assay method [0.1 M Tris (pH 8.0) with 0.2 mM DTNB, 400  $\mu$ M AcCoA, and 7  $\mu$ M AcAcCoA]. Each mixture was then passed through a G50 centrifugal column equilibrated with 0.1 M Tris (pH 8.0) to remove any residual unbound hymeglusin, and  $A_{280}$  was measured to confirm the comparability of the protein concentration of each sample.

Neutralized hydroxylamine (1 mM) was added to each sample. Activity assays were performed at the indicated incubation time points over a 1 h period.

**Crystallization, Collection of Diffraction Data, Structure Determination, Refinement, and Analysis.** *E. faecalis* mvaS was crystallized by vapor diffusion of hanging drops at 20 °C. In our protocol, 1  $\mu$ L of the protein solution (5 mg/mL) was mixed with 1  $\mu$ L of the reservoir solution [0.1 M Bis-Tris (pH 6.3–6.5), 0.2 M NaCl, and 23% (w/v) polyethylene glycol 3350] that had been previously diluted with an equal volume of doubly distilled H<sub>2</sub>O. Block-shaped crystals appeared after 2 days and continued to grow in size over the course of 1–2 weeks. Crystals were harvested and flash-cooled in a cryoprotectant solution of reservoir buffer in which the polyethylene glycol 3350 concentration had been increased to 30% (w/v). CocrySTALLIZATION was achieved by adding hymeglusin (final concentration of 0.5 mM) to a small volume of purified mvaS protein, prior to the establishment of crystallization drops as described above.

Monochromatic X-ray diffraction data were collected from single crystals at –173 °C using beamline 22-BM of the Advanced Photon Source, Argonne National Laboratory (Table 1). Upon the completion of data collection, the individual reflections were indexed, integrated, merged, and scaled using HKL2000.<sup>15</sup> Initial phase information was obtained for both structures presented here by molecular replacement using phenix.automr.<sup>16</sup> Chain A of a previously determined ligand-free *E. faecalis* mvaS structure [Protein Data Bank (PDB) entry 1X9E] was used as a search model.<sup>17</sup> The highest-scoring solution for this crystal system contained an mvaS tetramer in the asymmetric unit; this corresponded to a Matthews coefficient of 2.21 Å<sup>3</sup>/Da and a solvent content of 44.23%.

Structural refinement was conducted using additional protocols as implemented within the PHENIX suite.<sup>16</sup> First, the initial molecular replacement model was subjected to parallel automated rebuilding using phenix.autobuild.<sup>16</sup> This partially refined model was then improved by individual coordinate and atomic-displacement factor refinement using phenix.refine,<sup>16</sup> which also allowed calculation of both  $2F_o - F_c$  and  $F_o - F_c$  difference electron density maps. These maps were used to iteratively improve the model by manual rebuilding in Coot,<sup>18</sup> followed by additional rounds of refinement as described above. Ordered solvent molecules were added according to the default criteria of phenix.refine and validated by manual inspection in Coot prior to model completion. A complete list of refinement statistics can be found in Table 1.

**Ligand Fitting.** A model for the hymeglusin ligand was generated using the PRODRG server,<sup>19</sup> and the corresponding molecular restraint files were generated with phenix.elbow.<sup>16</sup> Examination of the initial  $F_o - F_c$  difference maps indicated unmodeled, contiguous density that corresponded to ordered hymeglusin at high occupancy within the active site of all four copies of mvaS within the asymmetric unit. Phenix.ligandfit<sup>16</sup> was then used to place and model a single hymeglusin molecule in each active site. Positional and atomic displacement factor refinement of the hymeglusin-bound mvaS structure was conducted as described above, with the exception that individual atom occupancy refinement was also used to model the hymeglusin bound at each mvaS active site independently.

**Table 1. Diffraction Data Collection and Structure Refinement Statistics**

	Data Collection <sup>a</sup>	
	<i>Ef</i> mvaS	<i>Ef</i> mvaS–hymeglusin
crystal		
beamline	APS 22-BM	APS 22-BM
wavelength (Å)	1.000	1.000
space group	<i>P</i> 2 <sub>1</sub>	<i>P</i> 2 <sub>1</sub>
cell dimensions	<i>a</i> = 109.53 Å <i>b</i> = 56.28 Å <i>c</i> = 123.89 Å $\beta$ = 100.02°	<i>a</i> = 108.33 Å <i>b</i> = 52.76 Å <i>c</i> = 117.58 Å $\beta$ = 99.51°
resolution (Å)	50.00–1.60	50.00–1.95
no. of reflections (unique)	1306891 (193904)	445318 (92792)
completeness (%)	98.5 (95.8)	96.8 (87.3)
redundancy (x-fold)	6.7	4.8
$\langle I \rangle / \langle \sigma I \rangle$	22.2 (3.6)	11.3 (2.6)
<i>R</i> <sub>merge</sub> (%) <sup>b</sup>	6.2 (45.6)	12.7 (42.1)
	Refinement	
PDB entry	3V4N	3V4X
no. of protein molecules per asymmetric unit	4	4
<i>R</i> <sub>work</sub> / <i>R</i> <sub>free</sub> (%) <sup>c</sup>	14.1/19.4	17.1/21.8
no. of atoms		
protein	11975	11862
ligand	not applicable	92
solvent	1494	1087
rmsd		
bond lengths (Å)	0.003	0.010
bond angles (deg)	0.72	1.25
<i>B</i> factor (Å <sup>2</sup> )		
protein	27.7	19.74
ligand	not applicable	32.34
solvent	35.9	24.95
coordinate error (Å)	0.400	0.200
phase error (deg)	20.3	21.8
Ramachandran plot (%)		
favored	97.7	97.4
allowed	2.3	2.6
outliers	0.0	0.0

<sup>a</sup>Numbers in parentheses are for the highest-resolution shell. <sup>b</sup>*R*<sub>merge</sub> =  $\sum_h \sum_i |I_i(h) - \langle I(h) \rangle| / \sum_h \sum_i I_i(h)$ , where *I<sub>i</sub>*(*h*) is the *i*th measurement of reflection *h* and  $\langle I(h) \rangle$  is a weighted mean of all measurements of *h*. <sup>c</sup>*R* =  $\sum_h |F_{\text{obs}}(h) - F_{\text{calc}}(h)| / \sum_h |F_{\text{obs}}(h)|$ . *R*<sub>cryst</sub> and *R*<sub>free</sub> were calculated from the working and test reflection sets, respectively. The test set constituted 10% of the total reflections not used in refinement.

## RESULTS

**Hymeglusin Inhibition of the Growth and Recovery of *E. faecalis* in the Absence of an Inhibitor.** The genetic disruption of *mvaS* and several other genes encoding mevalonate pathway enzymes has been demonstrated to block growth of *Streptococcus pneumoniae*.<sup>20</sup> To more specifically test the consequences of *mvaS* inhibition and the consequent restriction of downstream polyisoprenoid metabolites on *E. faecalis* growth, cells were incubated at 37 °C in LB either supplemented with 25  $\mu$ M hymeglusin or without inhibitor. Cells maintained in the presence of inhibitor exhibited no growth over the 5 h course of the experiment. In the absence of an inhibitor, the cells reached a growth curve inflection point at 0.7 h (Figure 1). A control sample of cells exhibiting no growth was pelleted and then resuspended in

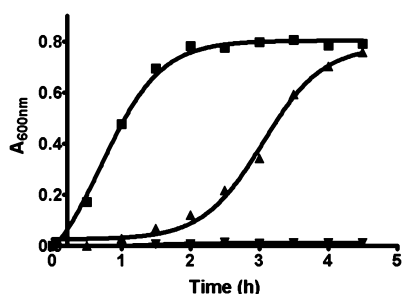


**Figure 1.** Recovery of the cellular growth of *E. faecalis* after removal of hymeglus. *E. faecalis* cells were grown in LB for 3 h at 37 °C in the presence or absence of 25  $\mu$ M hymeglus. Cells were pelleted, then resuspended in fresh LB, and again incubated at 37 °C. The absorbance was measured at 600 nm. The traces correspond to LB prior to cell pelleting followed by post-resuspension growth in LB (■), hymeglus and LB followed by post-resuspension LB (▲), and hymeglus and LB followed by post-resuspension hymeglus and LB (▼). The individual time points are averages of data from three experiments performed in parallel. Curves represent nonlinear regression fits of the data to a sigmoidal equation (GraphPad Prism 4). Inflection times and error estimates are listed in Table 2.

fresh LB in the absence of an inhibitor. These cells reached a growth curve inflection point at 3.1 h (Figure 1 and Table 2). The observations indicate that the putative adduct of hymeglus to mvaS can slowly be hydrolyzed to restore enzyme activity and the pool of essential polyisoprenoid metabolites. In contrast with these observations for *E. faecalis*, animal cells require only 1 h to exhibit a 50% rebound from inhibition.<sup>7</sup> Such observations would be compatible with the hypothesis of different hydrolysis rates for inhibitor adducts to animal HMG-CoA synthase versus bacterial mvaS.

**Time-Dependent Hymeglus Inactivation of *E. faecalis* mvaS.** Ambiguities in the nature of hymeglus inhibition of animal HMG-CoA synthase<sup>6,7</sup> were resolved by the results of Rokosz et al.<sup>8</sup> Work with purified recombinant human HMG-CoA synthase clearly indicated time-dependent inactivation. In contrast, the nature of hymeglus inhibition of bacterial mvaS has not been studied in detail. A basic kinetic characterization of purified *E. faecalis* mvaS [ $V_m$  = 10 units/mg (corresponding to  $k_{cat}$  = 6.9 s<sup>-1</sup>);  $K_{mAcCoA}$  = 350  $\mu$ M;  $K_{mAcCoA}$  = 10  $\mu$ M] has been reported previously,<sup>21</sup> but the scope of that

report did not include work on mvaS inhibitors or inactivators. To directly test the efficacy of hymeglus as an inhibitor, homogeneous *E. faecalis* mvaS was incubated with this compound at 18 °C with concentrations ranging from 75 to 600 nM. In each sample, a time-dependent loss of activity was observed (Figure 2), with >95% inhibition achieved at extended incubation times. These results suggest hymeglus inactivation of the enzyme by formation of a covalent adduct between the inhibitor and protein, as observed with the animal enzyme. Inactivation follows first-order kinetics, and the double-reciprocal replot of apparent  $k_{inact}$  values as a function of hymeglus concentration indicates saturable binding and provides estimates of a  $K_I$  of 606 nM and a  $k_{inact}$  of 2.75 min<sup>-1</sup> (inset of Figure 2 and Table 2). Nonlinear regression analysis of the primary data indicates a  $K_I$  of 700  $\pm$  18.5 nM and a  $k_{inact}$  of 3.5  $\pm$  0.6 min<sup>-1</sup> (Table 2). A partition ratio of 11.7  $\pm$  0.6 characterizes inactivation of mvaS by hymeglus. In comparison, inhibition of human HMG-CoA synthase by hymeglus is characterized by a  $K_I$  of 53.7 nM and a  $k_{inact}$  of 1.06 min<sup>-1</sup>.<sup>8</sup>

**Recovery of the Activity of Hymeglus-Inactivated mvaS and Human HMG-CoA Synthase upon Treatment with Hydroxylamine.** Neutralized hydroxylamine disrupts the thioester adducts of the HMG-CoA synthase reaction intermediates in which the acyl groups of acetyl-CoA or HMG-CoA are linked to the active site cysteine.<sup>22</sup> In hymeglus-inactivated *E. faecalis* mvaS or human HMG-CoA synthase, any thioester adduct formed between the  $\beta$ -lactone inhibitor and the active site cysteine should also be disrupted if it is accessible to an aqueous solution of hydroxylamine. When the resulting hydroxamic acid derivative of hymeglus is released from the active site cavity, enzyme activity could, in principle, be restored. This possibility was tested by incubation of hymeglus-inactivated bacterial and human enzymes with 1 mM hydroxylamine. Substantial activity was restored at a rate for the human enzyme (0.0097  $\pm$  0.0001 milliunit/min) that was 8-fold higher than that measured for the *E. faecalis* enzyme (0.0012  $\pm$  0.0002 milliunit/min) (Table 2). These results are compatible with the hypothesis that, for *E. faecalis* mvaS, the enzyme-S-hymeglus thioester adduct is less accessible to hydroxylamine in aqueous solvent than the corresponding adduct formed using human HMG-CoA synthase.

**Table 2.** Hymeglus Inhibition of *E. faecalis* and Human HMG-CoA synthase<sup>a</sup>

sample or enzyme	time to growth curve inflection point (h)	inactivation kinetic parameters	rate of activity restoration by 1 mM hydroxylamine (milliunit of activity recovered/min)
<i>E. faecalis</i> cells	0.71 $\pm$ 0.03		
<i>E. faecalis</i> cells with hymeglus	3.05 $\pm$ 0.04		
<i>E. faecalis</i> mvaS nonlinear fit method		$K_I$ = 700 $\pm$ 18.5 nM $k_{inact}$ = 3.5 $\pm$ 0.6 min <sup>-1</sup> $k_{inact}/K_I$ = 0.0050 $\pm$ 0.0016 nM <sup>-1</sup> min <sup>-1</sup>	0.0012 $\pm$ 0.0002
graphical method		$K_I$ = 606 nM $k_{inact}$ = 2.75 min <sup>-1</sup> $k_{inact}/K_I$ = 0.0045 nM <sup>-1</sup> min <sup>-1</sup>	
human HMGCS <sup>b</sup>		$K_I$ = 53.7 nM $k_{inact}$ = 1.06 min <sup>-1</sup> $k_{inact}/K_I$ = 0.0197 nM <sup>-1</sup> min <sup>-1</sup>	0.0097 $\pm$ 0.0001

<sup>a</sup>Experimental details are provided in the legends of Figures 1 and 2 and Experimental Procedures. <sup>b</sup>Values reported by Rokosz et al.<sup>8</sup>



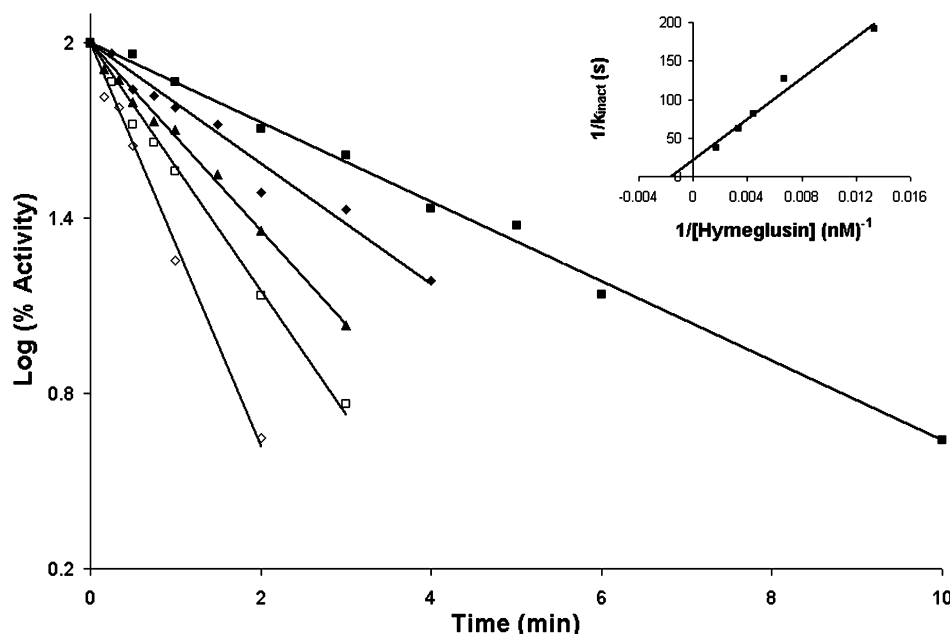


**Figure 2.** Time-dependent inactivation of *E. faecalis* HMG-CoA synthase/mvaS by hymegeglusin. Hymegeglusin was incubated with HMGCS/mvaS protein for the indicated times prior to addition of acetyl-CoA and DTNB. After a baseline level of 412 nm absorbance had been recorded, acetoacetyl-CoA was added to initiate the activity assay. Reaction mixtures contained 100 mM Tris-HCl (pH 8.0), 0.2 mM DTNB, 400  $\mu$ M Ac-CoA, 7  $\mu$ M acetoacetyl-CoA, and 2  $\mu$ g/mL enzyme. A semilog plot of percent HMGCS activity vs time is shown. Hymegeglusin concentrations of 75 (■), 150 (◆), 225 (▲), 300 (□), and 600 nM (◇) were used. Progress curves were fit to a linear model with  $R^2$  values of  $>0.97$ . The inset is a replot of the reciprocal of the apparent  $k_{\text{observed}}$  value (derived from  $t_{1/2}$  values of data sets depicted in the main figure) vs the reciprocal of hymegeglusin concentration. Intercepts on the  $x$  and  $y$  axes were used to determine a  $K_i$  of 606 nM and a  $k_{\text{inact}}$  of  $2.75 \text{ min}^{-1}$ , respectively. Nonlinear regression fits to the primary data were also performed (GraphPad Prism 4) and give a  $K_i$  of  $700 \pm 18.5 \text{ nM}$  and a  $k_{\text{inact}}$  of  $3.5 \pm 0.6 \text{ min}^{-1}$  (Table 2).

**Crystallographic Analysis of Hymegeglusin Bound to mvaS.** To further test this hypothesis, attempts were made to determine the structure of the hymegeglusin–mvaS adduct, which would provide additional information about the access of solvent to the active site cysteine when the hymegeglusin aliphatic chain occupies the active site cavity. Previous studies have established crystallization conditions for *E. faecalis* mvaS, which were used at that time to determine its structure both free and bound to the substrate acetoacetyl-CoA.<sup>17</sup> Although initial attempts to reproduce these crystals with the enzyme preparation described here were unsuccessful, an alternative crystal form was identified (Experimental Procedures). This novel crystal form was characterized by a change to a lower-symmetry space group (from  $I222$  to  $P2_1$ ) but with an increase in apparent resolution (from 2.4 to 1.6 Å) for the unbound enzyme. Using these crystals, a structure of mvaS was determined and refined to  $R_{\text{work}}$  and  $R_{\text{free}}$  values of 14.1 and 19.4%, respectively. This structure consists of four crystallographically unique copies of the enzyme within the asymmetric unit (Figure S1 of the Supporting Information and Table 1). By contrast, the previously determined structure of the same enzyme contained two polypeptides within its asymmetric unit.<sup>17</sup>

Diffraction quality samples were also obtained from *E. faecalis* mvaS that had been briefly incubated with an equimolar concentration of hymegeglusin immediately prior to establishment of the crystallization drops. These crystals of hymegeglusin-bound mvaS displayed only minor changes in cell constants when compared to those of the unbound enzyme and diffracted synchrotron X-rays to 1.95 Å limiting resolution (Table 1). After the collection of a nearly complete data set, the corresponding structure was determined by molecular replace-

ment and refined to  $R_{\text{work}}$  and  $R_{\text{free}}$  values of 17.1 and 21.8%, respectively (Figure 3 and Table 1). Examination of both  $2F_o - F_c$  and  $F_o - F_c$  difference electron density maps following initial rounds of refinement revealed the presence of largely contiguous, unmodeled density within the active site cavity for all four crystallographically unique copies of mvaS present within the asymmetric unit (Figure S2 of the Supporting Information). The extended nature of this density was consistent with the branched, aliphatic tail group of hymegeglusin. Furthermore, it was contiguous with the active site Cys<sup>111</sup> side chain in all four copies; this was indicative of a covalent adduct that would be anticipated following hymegeglusin modification of mvaS.

The readily interpretable nature of this unmodeled density allowed accurate placement of a single hymegeglusin ligand in each active site (Figure 3A). Comparison of the hymegeglusin conformations in all four active sites revealed that the ligand bound in essentially identical orientations with respect to mvaS (Figure 3B and Figures S2 and S3 of the Supporting Information). In particular, superposition of all four hymegeglusin chains within the refined structure yielded an average overall rmsd value of 0.72 Å across the entire ligand molecule. Interestingly, whereas the regions of the hymegeglusin molecules involved in covalent linkages to the Cys<sup>111</sup> thiolates superimpose quite well with one another, areas of greater conformational variability between the ligands bound at different mvaS active sites are found in the distal regions of the inhibitor. This is most likely because this region of hymegeglusin is quasi-linear and aliphatic in nature and (aside from the terminal carboxylate) lacks hydrogen bond donors and acceptors or other noteworthy structural features that

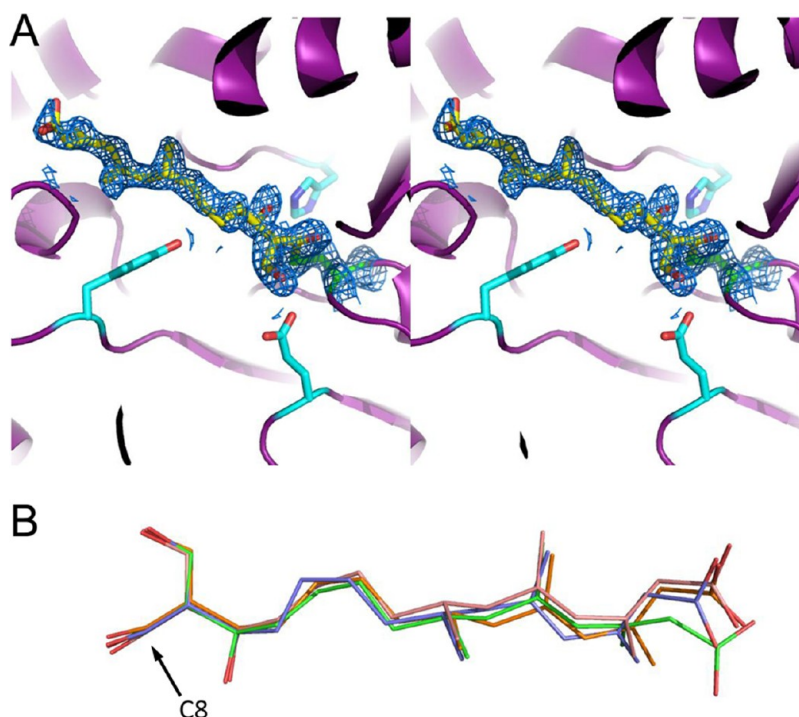


**Figure 3.** 1.95 Å structure of *E. faecalis* mvaS covalently modified by hymegeglusin. Crystals of *E. faecalis* mvaS that had been briefly incubated with hymegeglusin were produced as described in Experimental Procedures and used to collect monochromatic diffraction data. Following structure solution by molecular replacement, electron density maps that allowed modeling of bound ligand in each of the four crystallographically independent active sites were calculated. (A) Stereoview of the mvaS active site for chain A. The protein backbone is depicted in cartoon format (purple), while the side chains of Glu<sup>79</sup>, Tyr<sup>143</sup>, and His<sup>233</sup> are shown as cyan sticks. The catalytic Cys<sup>111</sup> is colored green, and carbon atoms of covalently bound hymegeglusin are colored yellow. The  $2F_o - F_c$  map (blue mesh at 1.1σ contour) of the refined structure corresponding to the Cys<sup>111</sup> thiolate-hymegeglusin adduct is also shown. (B) Overlay of hymegeglusin molecules as modeled in chains A–D, colored blue, green, orange, and red, respectively. The position of C8, which forms a covalent bond with the thiolate sulfur derived from Cys<sup>111</sup>, is denoted with an arrow. Additional information for all four active sites can be found in Figures S2–S4 of the Supporting Information.

might otherwise significantly restrict its conformation toward the entrance of the mvaS catalytic cleft.

The tubelike nature of the *Ef* mvaS active site channel allows nearly the entire hymegeglusin molecule to be buried within the cavity upon binding. On average, 381.4 Å<sup>2</sup> of surface area are buried through formation of the enzyme–inhibitor complex. This corresponds to approximately 84% of the total surface area available within the hymegeglusin molecule. Despite the fact that a large portion of hymegeglusin is aliphatic, two key polar interactions between its various functional groups and mvaS side chains stand out (Figure S4 of the Supporting Information). These are hydrogen bonds between the side chain Ne2 atom of His<sup>233</sup> and the O6 alcohol group of hymegeglusin (2.6 Å distance), and the side chain carboxylate of Glu<sup>79</sup> and the O5 alcohol of the inhibitor (2.9 Å distance). Previous kinetic and structural studies have consistently suggested that Glu<sup>79</sup> functions as a general acid/base during catalysis.<sup>17,22–24</sup> His<sup>233</sup> has also been assigned a role as a general acid/base during the condensation partial reaction of HMG-CoA synthesis;<sup>24</sup> however, it is also worth noting this residue contributes to binding of the second substrate, AcAc-CoA, by forming hydrogen bonds to its acetoacetyl group.<sup>22–24</sup> Similar interactions have also been described for His<sup>247</sup> and Glu<sup>48</sup> of the *B. juncea* HMG-CoA synthase in its hymegeglusin-bound state.<sup>10</sup> This further emphasizes the highly conserved nature of these specific side chains and their contributions to HMG-CoA synthase function across diverse evolutionary lineages.

**Differences in Active Site Accessibility between the Eukaryotic and Prokaryotic Synthases Explain the**

**Altered Stability of Their Hymegeglusin Adducts.** While *Ef* mvaS and the human and plant synthases are only approximately 27 and 28% identical, respectively, their overall folds are quite similar (Figure 4A), and all active site residues with clearly defined function are conserved. This conservation of mechanism is reflected in the analogous pairs of interactions formed between key enzyme side chains and the polar groups of the inhibitor hymegeglusin, as mentioned above. Nevertheless, the conserved nature of the active site residues provided no insight regarding the differences in kinetic inactivation or hydroxylamine reactivation of mvaS versus its eukaryotic counterpart (Table 2). This suggested that regions at the active site periphery instead may be responsible for these differences.

Indeed, an immediate and striking difference between the *Ef* mvaS and eukaryotic (*B. juncea*) HMG-CoA synthase involves the nature of the entrances to their respective active site cavities (Figure 4). The plant enzyme is characterized by a relatively wide cavity that is reminiscent of a triangular or pyramidal-shaped funnel, with the bound hymegeglusin laying flat against one its internal faces and extending nearly 16 Å into the catalytic core. For the purposes of illustration, the Cβ atom of Lys<sup>256</sup> serves as a convenient landmark for defining boundaries of the active site funnel, because it lies only 3.2 Å from the hymegeglusin carboxylate. Using this as a guide, the approximate dimensions of the funnel opening are 15.6 Å (Lys<sup>256</sup> to Cγ1 of Val<sup>204</sup>), 17.2 Å (Lys<sup>256</sup> to Cβ of Lys<sup>34</sup>), and 20.2 Å (Lys<sup>256</sup> to Cβ of Pro<sup>155</sup>). It is particularly notable that the catalytic cysteine (Cys<sup>117</sup>), which participates in the thioester bond that

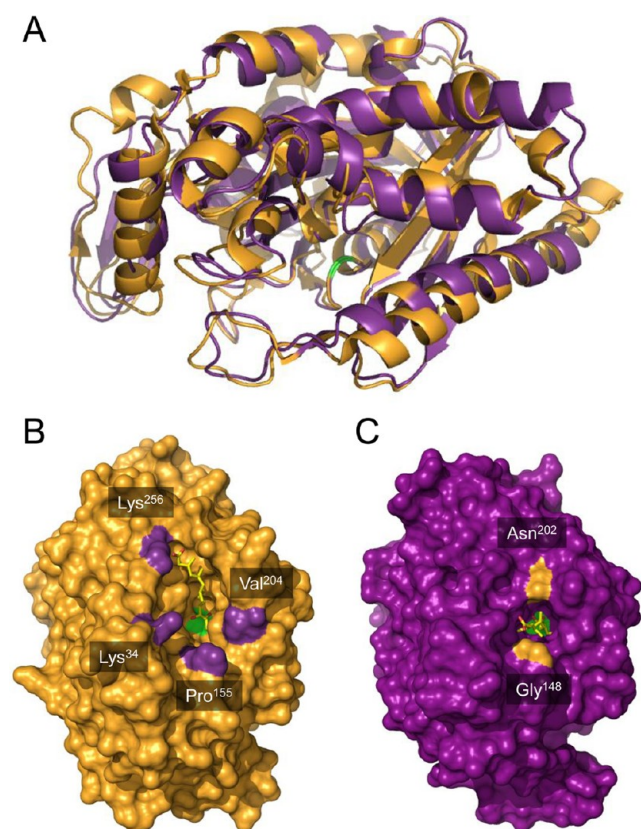


**Figure 4.** Comparison of hymeglusins-bound structures of eukaryotic HMG-CoA synthase and bacterial mvaS. (A) Crystal structure of hymeglusins-bound *B. juncea* HMG-CoA synthase (PDB entry 2F9A, orange cartoon) superimposed with that of hymeglusins-bound *E. faecalis* mvaS (PDB entry 3V4X, purple cartoon). Positions of the respective catalytic cysteine residues are colored green. (B) *B. juncea* HMG-CoA synthase shown as a molecular surface in an orientation identical to that in panel A. Bound hymeglusins are shown as a yellow ball and stick. The positions of landmark residues that define the boundaries of the active site entrance are indicated and colored purple. (C) *E. faecalis* mvaS shown as a molecular surface in an orientation identical to that in panel A. Bound hymeglusins are shown as a yellow ball and stick. The positions of landmark residues that define the boundaries of the active site entrance are indicated and colored orange.

covalently traps the inhibitor in place, has otherwise unrestricted access to the bulk solvent via the unoccupied side of this funnel.

In contrast, the *Ef* mvaS entrance is far more restricted and resembles a tunnel or tube. In this case, the backbone O of Gly<sup>148</sup> can be used as a landmark as it lies only 4.8 Å from the hymeglusins carboxylate. While this tunnel extends nearly 16 Å into the catalytic core, its opening is only 9.4 Å in diameter (as measured from Gly<sup>148</sup> to the side chain amide of Asn<sup>202</sup>). Because of this, covalently linked hymeglusins appears to be capable of quite effectively occluding the access of bulk solvent to the *Ef* mvaS catalytic Cys<sup>111</sup>. Thus, consideration of these architectural differences at the respective active site peripheries provides a structural explanation for the ~8-fold slower recovery of activity upon hydroxylamine treatment for mvaS relative to the eukaryotic synthase (Table 2).

## DISCUSSION

Hymeglusins has been recognized and described as a potent, covalent inhibitor of HMG-CoA synthases from bacterial, plant,

and animal origin. While inhibition of human HMG-CoA synthase by this fungal polyketide has been studied in some detail,<sup>8</sup> relatively little information is available regarding the specific nature of hymeglusins's effects on the bacterial synthase. This prompted us to conduct our study, which investigated the kinetic parameters of inactivation of mvaS by hymeglusins both in live *E. faecalis* cells and in vitro. Despite a common mode of inactivation (i.e., covalent modification), we observed significant differences in a number of biochemical parameters between the human and bacterial synthases (Table 2). The human synthase is far more sensitive to inhibition by hymeglusins, as demonstrated by its 10-fold lower  $K_i$  value (53.7 nM) relative to that of mvaS (700 nM). This differential affinity influences the inactivation efficiency ( $k_{\text{inact}}/K_i$ ), which is higher for human HMG-CoA synthase (0.0197) than for *E. faecalis* mvaS (0.0050) (Table 2). However, significant differences between both the formation and the stability of hymeglusins-synthase adducts were seen. Hymeglusins-mediated inactivation manifests itself at a faster rate in bacterial mvaS than in human HMG-CoA synthase. Inactivation is also more transient (shorter in duration) for the human enzyme than for its bacterial counterpart. Apparent differences in the duration of inactivation are in accord with the approximately 8-fold slower activity recovery rate following hydroxylamine treatment for inhibited *E. faecalis* mvaS when compared to human HMG-CoA synthase. This strongly suggested that differences in active site solvent accessibility contributed to the differences between inactivation of the human and bacterial enzymes.

We obtained further insight into the basis for hymeglusins inhibition of *E. faecalis* mvaS through structural studies of the covalently modified enzyme. In doing so, a novel crystal form of *E. faecalis* mvaS was identified that provided improved diffraction limits when compared to that previously reported for the same enzyme.<sup>17</sup> Interestingly, the unit cell parameters for the crystal system described here match exceedingly well those reported by Campobasso and colleagues for *Staphylococcus aureus* mvaS (which is ~60% identical) when bound to its substrate acetoacetyl-CoA.<sup>23</sup> Comparison of the hymeglusins-bound *E. faecalis* mvaS structure presented here to those of either the *E. faecalis*<sup>17</sup> or *S. aureus*<sup>23</sup> enzyme bound to various CoA derivatives reveals that the aliphatic tail of hymeglusins occupies a region within the enzymes' relatively long, active site tunnel that is largely identical to that of the pantothenic acid moiety of CoA in these closely related structures (Figure 5). That said, it is noteworthy that the hymeglusins tail is completely extended and not kinked as in the distal, reactive region of CoA. This elongated conformation allows the covalent inhibitor to effectively bypass the hydrophobic crevice formed by Tyr<sup>205</sup>, Met<sup>239</sup>, and Tyr<sup>306</sup> of mvaS, which itself accommodates the reactive cysteine/thiol-containing functionality of the coenzyme. Intriguingly, this stands in contrast to what is observed for the *B. juncea* HMG-CoA synthase when it is bound to hymeglusins, acetyl-CoA, or HMG-CoA.<sup>10</sup> Here, the aliphatic hymeglusins chain actually follows, rather than bypasses, the kink found in the distal region of the CoA (Figure 6). In doing so, the terminal region of the hymeglusins chain binds to an opposing face of the funnel-shaped entrance to the enzyme's active site versus what is seen for either CoA derivative. Such a dramatic difference in ligand binding mode is not possible within the bacterial enzyme, as its tunnel-shaped active site entrance imposes significant structural restraints on any inhibitors or substrates that occupy this region. One important consequence of these architectural



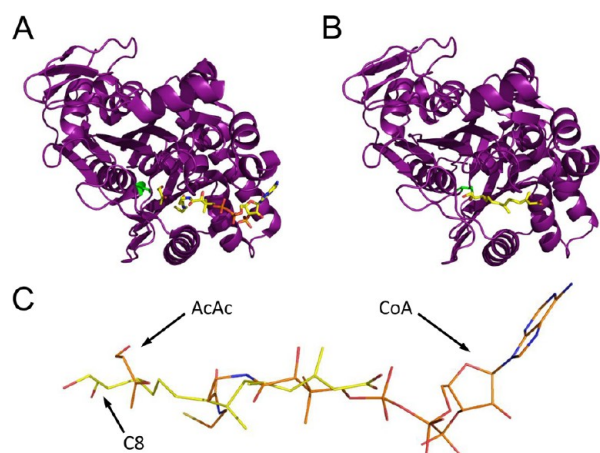


**Figure 5.** Comparison of *E. faecalis* mvaS structures bound to either acetoacetate and CoA or hyme-gluslin. (A) Chain B from the structure of mvaS bound to acetoacetate and CoA (PDB entry 1YSL). The polypeptide is shown as a purple cartoon, while the ligands are shown in ball and stick format. The catalytic cysteine residue is colored green. (B) Chain A from the structure of mvaS bound to hyme-gluslin (PDB entry 3V4X). (C) Superposition of the CoA and hyme-gluslin structures as they lie within the mvaS active site. Note that the aliphatic tail of hyme-gluslin largely occupies the same position as the pantothenic acid moiety of CoA. The positions of acetoacetate (AcAc), coenzyme A (CoA), and C8 of hyme-gluslin (C8) are denoted with arrows.

differences among HMG-CoA synthases across various kingdoms of life is that the active sites of the eukaryotic forms appear to have relatively free access to bulk solvent, whereas their bacterial counterparts are more restricted. While the physiological relevance of this difference is not clear at this time, it does provide a rational basis for the notably altered kinetic inactivation parameters reported here (Figures 1 and 2 and Table 2) and elsewhere.<sup>8</sup> Furthermore, it also strongly suggests that inhibitors that are highly selective for the bacterial enzymes over their human homologue can be discovered, optimized, and developed.

In the description of the eukaryotic HMGCS–hyme-gluslin adduct structure,<sup>10</sup> it was noted that the active site glutamate hydrogen bonds to the C2 hydroxyl of the ring-opened inactivator. On the basis of such structural observations, additional function for the catalytic glutamate in catalysis of thioester hydrolysis was proposed. Such a hypothesis can be discounted on the basis of results of direct functional tests of the thioester hydrolysis partial reaction.<sup>22</sup> Alanine substitution of the catalytic glutamate produces a mutant enzyme that is unimpaired in catalysis of this partial reaction. Neither  $V_m$  nor  $K_m$  values are substantially different from those of the wild-type enzyme. In contrast, however, this mutant exhibits a >5 orders of magnitude diminution of the overall reaction (Scheme 1) in comparison with the wild-type enzyme. This confirms the previous functional assignment of this active site glutamate in the condensation partial reaction.<sup>22,24</sup>

In addition to hyme-gluslin's ability to inactivate both prokaryotic and eukaryotic HMG-CoA synthase, we recently demonstrated the ability of epoxide-containing molecules to inhibit the eukaryotic enzyme.<sup>25</sup> Cerulenin is an antibiotic that inhibits  $\beta$ -ketoacyl acyl carrier protein synthases, the bacterial fatty acid-condensing enzymes.<sup>26</sup> Its epoxide moiety reacts with the active site cysteine to form a stable thioether adduct. These enzymes as well as HMG-CoA synthases are members of the family of initial condensation enzymes, and they exhibit

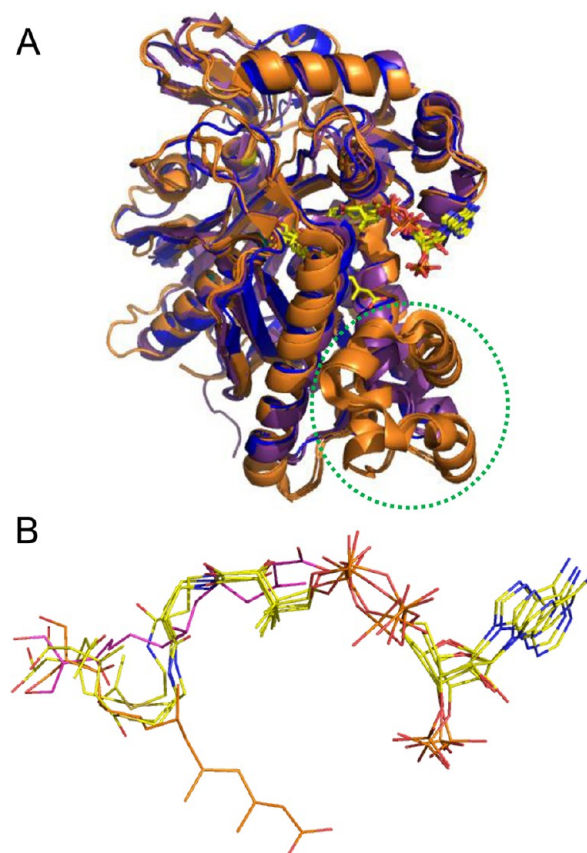


**Figure 6.** Comparison of available ligand-bound structures for *E. faecalis* and *S. aureus* mvaS and *B. juncea* HMG-CoA synthases. (A) Superposition of enzyme monomers from *E. faecalis* mvaS bound to hyme-gluslin (PDB entry 2V4X) and acetyl-CoA (PDB entry 1YSL, chain B), *S. aureus* mvaS bound to acetoacetyl-CoA (PDB entry 1TXT, chain A), and *B. juncea* HMG-CoA synthase bound to hyme-gluslin (PDB entry 2F9A), acetyl-CoA (PDB entry 2FA3), and HMG-CoA (PDB entry 2FA0). The *E. faecalis* and *S. aureus* structures are colored purple and blue, respectively, while the *B. juncea* structures are colored orange. The location of the helical insertion domain that is found only in the eukaryotic enzyme is highlighted with a dashed green circle. The positions of the bound ligands and inhibitors are shown in ball and stick format. Note that each of these ligands or inhibitors adopts the same positional conformation, except for hyme-gluslin when bound to *B. juncea* HMG-CoA synthase. Instead, this inhibitor binds to an opposing face of the active site funnel when compared to the CoA derivatives. (B) Magnified views of the positions of each of the ligands and inhibitors from panel A as they lie within the superimposed enzyme active sites. All CoA-derived ligands are shown colored with their carbon atoms in yellow, while hyme-gluslin as found in the *E. faecalis* and *B. juncea* enzymes is colored with purple and orange carbon atoms, respectively.

considerable structural and functional homology. On this basis, it seemed reasonable to test cerulenin against HMG-CoA synthase; the human enzyme proves to be sensitive to this inhibitor, displaying time-dependent inactivation.<sup>25</sup> *S. aureus* mvaS also exhibits time-dependent inactivation by cerulenin (I. Misra and H. M. Miziorko, unpublished results). Ceestatin, a novel epoxide-containing compound, inhibits hepatitis C virus replication via a mechanism attributed to its demonstrated time-dependent inactivation of eukaryotic (human) HMG-CoA synthase.<sup>25</sup> While these epoxide inhibitors are effective, in vitro, at concentrations higher than those required for hyme-gluslin, the thioether adducts that presumably form upon active site



cysteine modification are not labile under the same physiological conditions that permit thioester adduct hydrolysis. This is particularly relevant in terms of potential anti-infective applications of hymeglusins and related compounds, because data presented here show that hymeglusins' effect on live bacterial cells is reversible on the order of hours (Figure 1 and Table 2). Thus, in any future work on the design or optimization of HMG-CoA synthase inhibitors, the chemical nature of the protein–inhibitor adduct should receive consideration. In this regard, the structural information available on enzyme–inhibitor complexes along with the characterized differences in kinetic inactivation parameters presented herein should prove to be a valuable asset moving forward.

## ■ ASSOCIATED CONTENT

### ■ Supporting Information

Four supplemental figures and their figure legends. This material is available free of charge via the Internet at <http://pubs.acs.org>.

## ■ AUTHOR INFORMATION

### Corresponding Author

\*H.M.M.: e-mail, [miziorkoh@umkc.edu](mailto:miziorkoh@umkc.edu). B.V.G.: e-mail, [geisbrecht@umkc.edu](mailto:geisbrecht@umkc.edu); School of Biological Sciences, University of Missouri—Kansas City, 5100 Rockhill Rd., Kansas City, MO 64110; telephone, (816) 235-2246; fax, (816) 235-5595.

### Author Contributions

D.A.S. and K.X.R. contributed equally to this work.

### Author Contributions

B.V.G. and H.M.M. shared supervision of this work.

### Funding

This work was supported in part by National Institutes of Health Grants AI071028 and AI090149 and the Marion Merrell-Dow Foundation.

### Notes

The authors declare no competing financial interest.

## ■ ACKNOWLEDGMENTS

Dr. Michael Greenspan (Merck) generously provided the hymeglusins used in these studies. Dr. Ila Misra (Medical College of Wisconsin) determined that hymeglusins is a time-dependent inactivator of *S. aureus* mvaS. We acknowledge generous technical assistance of Drs. Rod Salazar, Andy Howard, and John Chrzas during X-ray diffraction data collection. Use of the Advanced Photon Source was supported by the U.S. Department of Energy, Office of Science, Office of Basic Energy Sciences, via Contract W-31-109-Eng-38. Data were collected at Southeast Regional Collaborative Access Team (SER-CAT) beamlines at the Advanced Photon Source, Argonne National Laboratory. A list of supporting member institutions may be found at <http://www.ser-cat.org/members.html>.

## ■ ABBREVIATIONS

HMG-CoA, 3-hydroxy-3-methylglutaryl-CoA; Ac-CoA, acetyl-CoA; AcAc-CoA, acetoacetyl-CoA; F244 (or 1233A), hymeglusins; mvaS, prokaryotic HMG-CoA synthase; HMGCS, eukaryotic HMG-CoA synthase; DTNB, dithiobisnitrobenzoic

acid; *Ef*, *E. faecalis*; LB, Luria-Bertani medium; rmsd, root-mean-square deviation.

## ■ REFERENCES

- (1) Aldridge, D. C., Giles, D., and Turner, W. B. (1971) Antibiotic 1233A: A fungal  $\beta$ -lactone. *J. Chem. Soc., Perkin Trans. 1* 23, 3888–3891.
- (2) Tomoda, H., Kumagai, H., Takahashi, Y., Tanaka, Y., Iwai, Y., and Omura, S. (1988) F-244 (1233A), a specific inhibitor of 3-hydroxy-3-methylglutaryl coenzyme A synthase: Taxonomy of producing strain, fermentation, isolation and biological properties. *J. Antibiot.* 41, 247–249.
- (3) Miziorko, H. M., and Behnke, C. E. (1985) Active-site-directed inhibition of 3-hydroxy-3-methylglutaryl coenzyme A synthase by 3-chloropropionyl coenzyme A. *Biochemistry* 24, 3174–3179.
- (4) Miziorko, H. M., and Behnke, C. E. (1985) Amino acid sequence of an active site peptide of avian liver mitochondrial 3-hydroxy-3-methylglutaryl-CoA synthase. *J. Biol. Chem.* 260, 13513–13516.
- (5) Omura, S., Tomoda, H., Kumagai, H., Greenspan, M. D., Yodkovitz, J. B., Chen, J. S., Alberts, A. W., Martin, I., Mochales, S., Monaghan, R. L., et al. (1987) Potent inhibitory effect of antibiotic 1233A on cholesterol biosynthesis which specifically blocks 3-hydroxy-3-methylglutaryl coenzyme A synthase. *J. Antibiot.* 40, 1356–1357.
- (6) Greenspan, M. D., Yodkovitz, J. B., Lo, C. Y., Chen, J. S., Alberts, A. W., Hunt, V. M., Chang, M. N., Yang, S. S., Thompson, K. L., Chiang, Y. C., et al. (1987) Inhibition of hydroxymethylglutaryl-coenzyme A synthase by L-659,699. *Proc. Natl. Acad. Sci. U.S.A.* 84, 7488–7492.
- (7) Greenspan, M. D., Bull, H. G., Yodkovitz, J. B., Hanf, D. P., and Alberts, A. W. (1993) Inhibition of 3-hydroxy-3-methylglutaryl-CoA synthase and cholesterol biosynthesis by  $\beta$ -lactone inhibitors and binding of these inhibitors to the enzyme. *Biochem. J.* 289 (Part 3), 889–895.
- (8) Rokosz, L. L., Boulton, D. A., Butkiewicz, E. A., Sanyal, G., Cueto, M. A., Lachance, P. A., and Hermes, J. D. (1994) Human cytoplasmic 3-hydroxy-3-methylglutaryl coenzyme A synthase: Expression, purification, and characterization of recombinant wild-type and Cys129 mutant enzymes. *Arch. Biochem. Biophys.* 312, 1–13.
- (9) Misra, I., Narasimhan, C., and Miziorko, H. M. (1993) Characterization of a Recombinant Cholesterologenic Isozyme and Demonstration of the Requirement for a Sulfhydryl Functionality in the Formation of the Acetyl-Enzyme Reaction Intermediate. *J. Biol. Chem.* 268, 12129–12136.
- (10) Pojer, F., Ferrer, J. L., Richard, S. B., Nagegowda, D. A., Chye, M. L., Bach, T. J., and Noel, J. P. (2006) Structural basis for the design of potent and species-specific inhibitors of 3-hydroxy-3-methylglutaryl CoA synthases. *Proc. Natl. Acad. Sci. U.S.A.* 103, 11491–11496.
- (11) Simon, E. J., and Shemin, D. (1953) The preparation of S-succinyl coenzyme A. *J. Am. Chem. Soc.* 75, 2520.
- (12) Geisbrecht, B. V., Bouyain, S., and Pop, M. (2006) An Optimized System for the Expression and Purification of Secreted Bacterial Proteins. *Protein Expression Purif.* 46, 23–32.
- (13) Barta, M. L., Skaff, D. A., McWhorter, W. J., Herdendorf, T. J., Miziorko, H. M., and Geisbrecht, B. V. (2011) Crystal structures of *Staphylococcus epidermidis* mevalonate diphosphate decarboxylase bound to inhibitory analogs reveal new insight into substrate binding and catalysis. *J. Biol. Chem.* 286, 23900–23910.
- (14) Skaff, D. A., and Miziorko, H. M. (2010) A visible wavelength spectrophotometric assay suitable for high-throughput screening of 3-hydroxy-3-methylglutaryl-CoA synthase. *Anal. Biochem.* 396, 96–102.
- (15) Otwinowski, Z., and Minor, W. (1997) Processing of X-ray Diffraction Data Collected in Oscillation Mode. *Methods Enzymol.* 276, 307–326.
- (16) Adams, P. D., Afonine, P. V., Bunkoczi, G., Chen, V. B., Davis, I. W., Echols, N., Headd, J. J., Hung, L. W., Kapral, G. J., Grosse-Kunstleve, R. W., McCoy, A. J., Moriarty, M. W., Oeffner, R., Read, R. J., Richardson, D. C., Richardson, J. S., Terwilliger, T. C., and Zwart, P. H. (2010) PHENIX: A Comprehensive Python-Based System for Macromolecular Structure Solution. *Acta Crystallogr. D* 66, 213–221.

- (17) Steussy, C. N., Vartia, A. A., Burgner, J. W., Sutherlin, A., Rodwell, V. W., and Stauffacher, C. V. (2005) X-ray Crystal Structures of HMG-CoA Synthase from *Enterococcus faecalis* and a Complex with Its Second Substrate/Inhibitor Acetoacetyl-CoA. *Biochemistry* 44, 14256–14267.
- (18) Emsley, P., Lohkamp, B., Scott, W. G., and Cowtan, K. (2010) Features and Development of Coot. *Acta Crystallogr. D* 66, 486–501.
- (19) Schuettkopf, A. W., and van Aalten, D. M. F. (2004) PRODRG: A Tool for High-throughput Crystallography of Protein-Ligand Complexes. *Acta Crystallogr. D* 60, 1355–1363.
- (20) Wilding, E. I., Kim, D. Y., Bryant, A. P., Gwynn, M. N., Lunsford, R. D., McDevitt, D., Myers, J. E., Jr., Rosenberg, M., Sylvester, D., Stauffacher, C. V., and Rodwell, V. W. (2000) Essentiality, expression, and characterization of the class II 3-hydroxy-3-methylglutaryl coenzyme A reductase of *Staphylococcus aureus*. *J. Bacteriol.* 182, 5147–5152.
- (21) Sutherlin, A., Hedl, M., Sanchez-Neri, B., Burgner, J. W., II, Stauffacher, C. V., and Rodwell, V. W. (2002) *Enterococcus faecalis* 3-hydroxy-3-methylglutaryl coenzyme A synthase, an enzyme of isopentenyl diphosphate biosynthesis. *J. Bacteriol.* 184, 4065–4070.
- (22) Chun, K. Y., Vinarov, D. A., Zajicek, J., and Mizioroko, H. M. (2000) 3-Hydroxy-3-methylglutaryl-CoA synthase. A role for glutamate 95 in general acid/base catalysis of C-C bond formation. *J. Biol. Chem.* 275, 17946–17953.
- (23) Campobasso, N., Patel, M., Wilding, I. E., Kallender, H., Rosenberg, M., and Gwynn, M. N. (2004) *J. Biol. Chem.* 279, 44883–44888.
- (24) Theisen, M. J., Misra, I., Saadat, D., Campobasso, N., Mizioroko, H. M., and Harrison, D. H. (2004) 3-Hydroxy-3-methylglutaryl-CoA synthase intermediate complex observed in “real-time”. *Proc. Natl. Acad. Sci. U.S.A.* 101, 16442–16447.
- (25) Peng, L. F., Schaefer, E. A., Maloof, N., Skaff, A., Berical, A., Belon, C. A., Heck, J. A., Lin, W., Frick, D. N., Allen, T. M., Mizioroko, H. M., Schreiber, S. L., and Chung, R. T. (2011) Ceestatin, a novel small molecule inhibitor of hepatitis C virus replication, inhibits 3-hydroxy-3-methylglutaryl-coenzyme A synthase. *J. Infect. Dis.* 204, 609–616.
- (26) Price, A. C., Choi, K. H., Heath, R. J., Li, Z., White, S. W., and Rock, C. O. (2001) Inhibition of  $\beta$ -ketoacyl-acyl carrier protein synthases by thiolactomycin and cerulenin. Structure and mechanism. *J. Biol. Chem.* 276, 6551–6559.